Antiresonance and bound states in the continuum in electron transport through parallel-coupled quantum-dot structures

2009 J. Phys.: Condens. Matter 21 175801

(http://iopscience.iop.org/0953-8984/21/17/175801)

J. Phys.: Condens. Matter **21** (2009) 175801 (8pp) doi:10.1088/0953-8984/21/17/175801

Antiresonance and bound states in the continuum in electron transport through parallel-coupled quantum-dot structures

Weijiang Gong[1], **Yu Han**[1] **and Guozhu Wei**[1,2,3]

[1] College of Sciences, Northeastern University, Shenyang 110004, People's Republic of China
[2] International Center for Material Physics, Acadmia Sinica, Shenyang 110015, People's Republic of China

E-mail: guozhuwei02@sina.com

Received 17 December 2008, in final form 9 March 2009
Published 30 March 2009
Online at stacks.iop.org/JPhysCM/21/175801

Abstract

In this paper we make a theoretical study of electron transport through a multi-quantum-dot system, in which the peripheral quantum dots of a one-dimensional chain are embodied in the two arms of an Aharonov–Bohm interferometer. It is found that, in the absence of magnetic flux, all the even molecule states of odd-numbered quantum-dot structures decouple from the leads and in even-numbered quantum-dot systems all the odd molecule states decouple from the leads, which indicates the formation of remarkable bound states in the continuum. Meanwhile, what is interesting is that apparent antiresonance occurs in electron transport through this structure, the positions of which are accordant with all even (odd) eigenenergies of the sub-molecule of the even (odd)-numbered quantum dots without the peripheral dots. All these results are efficiently modified by the presence of magnetic flux through this system.

(Some figures in this article are in colour only in the electronic version)

1. Introduction

The well-known bound state in continuum (BIC) was first proposed by von Neumann and Wigner for certain spatially oscillating attractive potentials [1]. Over the past decades this topic has been extensively investigated in the field of quantum physics, and a number of theoretical studies of BIC have been reported [2, 3]. Stillinger and Herrick generalized this problem and analyzed the formation of BICs in a two-electron model, despite the interaction between electrons [2]. The occurrence of BICs was also discussed in a system of coupled Coulomb channels and, in particular, in a hydrogen atom in a uniform magnetic field [4]. Besides, the formation of a BIC becomes of great interest in the study of various systems in relation to such matters as the photodetachment of electrons from negative ions and the spontaneous emission of photons from atoms in photonic crystals [5, 6]. For unstable multilevel systems bound states inside the continuum have been studied based on the N-level Friedrichs model [7]. Wang *et al* reported that BICs in solid state electron systems can be induced by the lattice structure [8].

Recently, the BIC phenomenon has also been shown to be present in electronic transport through mesoscopic structures, so accordingly becomes a main concern in mesoscopic physics. For instance, Capasso *et al* reported the experimental evidence for BICs in semiconductor heterostructures grown by molecular beam epitaxy [9]. In addition, the formation of BICs in mesoscopic systems has also received much attention from theoretical physicists [10–15], and there are theoretical works showing the formation of bound states in a four-terminal junction and in a ballistic channel with intersections [10, 11]. The appearance of BICs has been predicted in quantum waveguides with serial stubs [12–14]. Recently, it was shown that in a one-dimensional semiconductor quantum wire with two identical adatom impurities, BICs arise even when the energy of the adatom impurity is located in a continuous one-dimensional energy miniband [16].

However, so far BICs have been little discussed in the context of electron transport through quantum-dot (QD) systems. As is known, mutually coupled multi-QD systems, in

[3] Author to whom any correspondence should be addressed.

comparison with a single-QD structure, exhibit more intricate electron transport behaviors because these systems provide more Feynman paths for electron transmission. Quantum interference of electron waves passing through different Feynman paths brings about abundant transport properties if the size of the multi-QD system is shorter than or comparable to the electron phase coherence length. In addition, multi-QD systems possess more tunable parameters than a single QD to manipulate the electronic transport behaviors. Typically, in parallel-coupled QD systems, by the presence of an appropriate magnetic flux or Rashba spin–orbit interaction, the couplings between the molecular states of the coupled QDs and leads can be adjusted, giving rise to the Fano effect [17–21]. Moreover, for some particular cases, some molecular state can decouple completely from the leads, so that the so-called BIC phenomenon comes into being. With this in mind, the occurrence of BICs has been investigated in parallel-coupled QD systems embedded in an Aharonov–Bohm (AB) interferometer, where the position and number of BICs are associated with the adjustment of the threading magnetic flux [22, 23]. Besides, some works show the coexistence of BIC and antiresonance induced by the degeneracy of eigenlevels of QDs in the QD ring [24]. According to this previous research, the existence of BICs plays an important role in the quantum interference of QD structures. Therefore, it is desirable to clarify the BICs in some typical coupled QD structures.

With the development of nanotechnology, it is feasible to fabricate coupled QDs, in particular a QD chain [25, 26]. Therefore we are now theoretically concerned with the electron transport properties of the this structure, by considering it embodied in an AB interferometer. We find that, in the absence of magnetic flux, all the even molecule states for odd-numbered QD structures decouple from the leads and in even-numbered QD systems all odd molecule states decouple from the leads, bringing about the formation of BICs. In previous works the even–odd effect also attracted much attention [27]. Interestingly, antiresonances also occur in electron transport through this structure, and their positions are in accord with all even (odd) eigenenergies of the sub-molecule of the even (odd)-numbered QDs without the peripheral QDs. Besides, the occurrence of BICs and antiresonance are efficiently modified by the presence of magnetic flux through this system.

The rest of the paper is organized as follows. In section 2, the model Hamiltonian to describe electron behavior in the multi-QD structure is first introduced. Then a formula for linear conductance is derived by means of the nonequilibrium Green function technique. In section 3, the calculated results regarding the conductance spectrum are shown. Then a discussion on the numerical results, particularly those concerning the occurrence of BICs and antiresonance, is given. Finally, the main results are summarized in section 4.

2. The theoretical model

The parallel multi-QD structure that we consider is schematically illustrated in figure 1(a). The electron motion in this system can be well described by a generalized Anderson impurity

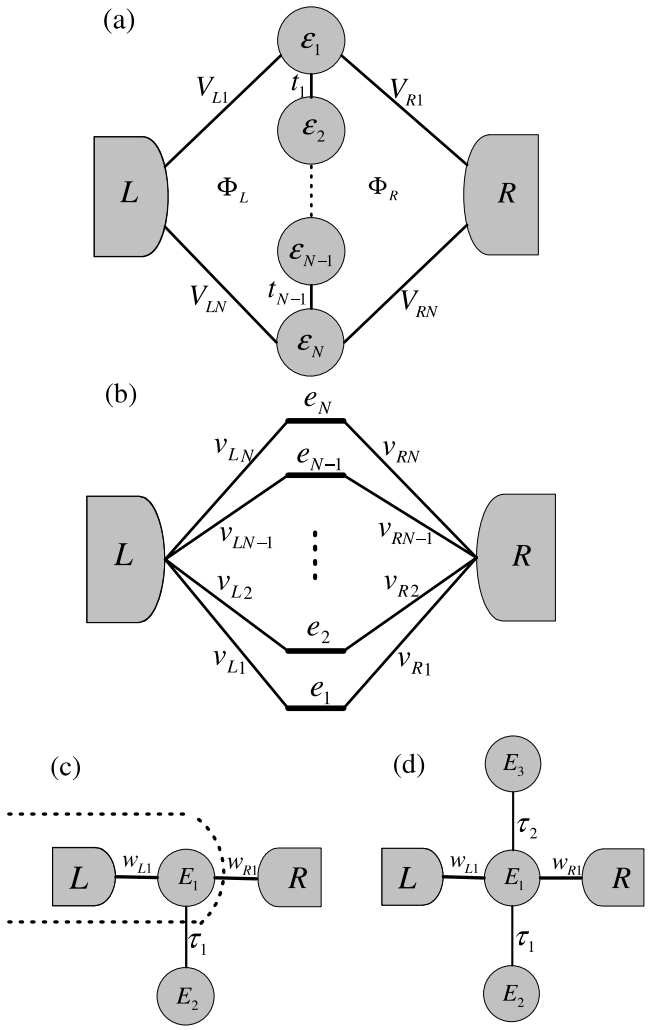

Figure 1. (a) Schematic of a QD chain embodied in an Aharonov–Bohm interferometer with two magnetic fluxes $\Phi_{\rm L}$ and $\Phi_{\rm R}$ through the subrings of this structure. (b) An illustration of the couplings between the molecule states of the QDs and the leads. (c), (d) Schematics of T-shaped QD structures.

Hamiltonian which reads

$$H = H_0 + H_{\rm T} + H_{\rm e-e}, \tag{1}$$

with

$$H_0 = \sum_{k\sigma\alpha\in{\rm L,R}} \varepsilon_{\alpha k} c^\dagger_{\alpha k\sigma} c_{\alpha k\sigma} + \sum_{j=1,\sigma}^{N} \varepsilon_j d^\dagger_{j\sigma} d_{j\sigma} + \sum_{\sigma,j=1}^{N-1} t_j d^\dagger_{j+1\sigma} d_{j\sigma} + {\rm h.c.},$$

$$H_{\rm T} = \sum_{\alpha k\sigma} V_{\alpha 1} d^\dagger_{1\sigma} c_{\alpha k\sigma} + \sum_{k\sigma} V_{\alpha N} d^\dagger_{N\sigma} c_{\alpha k\sigma} + {\rm h.c.},$$

$$H_{\rm e-e} = \sum_j U_j n_{j\uparrow} n_{j\downarrow},$$

where $c^\dagger_{\alpha k\sigma}(c_{\alpha k\sigma})$ is an operator to create (annihilate) an electron of the continuous state k in lead-α, and $\varepsilon_{\alpha k}$ is the corresponding single-particle energy, with σ being the spin index. $d^\dagger_{j\sigma}(d_{j\sigma})$ is the creation (annihilation) operator of an

electron in QD-j, and ε_j denotes the corresponding electron level. t_j is the interdot coupling coefficient between the jth and the $(j+1)$th QDs. $H_{\rm T}$ describes the electron tunneling between the leads and QDs; in the case of symmetrical dot–lead coupling $V_{\alpha j}$, the dot–lead coupling coefficients can be written explicitly as $V_{\rm L1} = V{\rm e}^{{\rm i}\phi_{\rm L}/2}$, $V_{\rm LN} = V{\rm e}^{-{\rm i}\phi_{\rm L}/2}$, $V_{\rm R1} = V{\rm e}^{-{\rm i}\phi_{\rm R}/2}$, and $V_{\rm RN} = V{\rm e}^{{\rm i}\phi_{\rm R}/2}$ with V being the dot–lead coupling strength. The magnetic flux, in the symmetric gauge, gives rise to the AB phase $\phi_\alpha = 2\pi\Phi_\alpha/\Phi_0$, where Φ_α is the magnetic flux threading the subrings and $\Phi_0 = hc/e$ is the flux quantum. The last term denotes the intradot Coulomb interaction.

In order to study the electron transport properties of this structure, the linear conductance in this system should be calculated, which is associated with the Green functions and takes the form of [28, 29]

$$\mathcal{G} = \frac{e^2}{h}\sum_\sigma {\rm Tr}[\Gamma^{\rm L} G^{\rm a}_\sigma(\omega)\Gamma^{\rm R} G^{\rm r}_\sigma(\omega)]_{\omega=\varepsilon_{\rm F}}. \tag{2}$$

$\Gamma^{\rm L}$, defined as $[\Gamma^{\rm L}]_{ij} = 2\pi V_{{\rm L}i}V^*_{{\rm L}j}\rho_{\rm L}(\omega)$, describes the coupling strength between the QDs and lead-L. We will ignore the ω-dependence of $\Gamma^{\rm L}$ since the electron density of states in lead-L, $\rho_{\rm L}(\omega)$, can usually be viewed as a constant. Similarly, we can define $[\Gamma^{\rm R}]$, the coupling strength between the QDs and lead-R. In equation (2) the retarded and advanced Green functions in Fourier space are involved. They are defined as follows: $G^{\rm r}_{jl,\sigma}(t) = -{\rm i}\theta(t)\langle\{d_{j\sigma}(t), d^\dagger_{l\sigma}\}\rangle$ and $G^{\rm a}_{jl,\sigma}(t) = {\rm i}\theta(-t)\langle\{d_{j\sigma}(t), d^\dagger_{l\sigma}\}\rangle$, where $\theta(x)$ is the step function. The Fourier transforms of the Green functions can be performed via $G^{\rm r(a)}_{jl,\sigma}(\omega) = \int_{-\infty}^{\infty} G^{\rm r(a)}_{jl,\sigma}(t){\rm e}^{{\rm i}\omega t}\,{\rm d}t$. These Green functions can be solved by means of the equation-of-motion method. By a straightforward derivation, we obtain the solution of the retarded Green function, which is written in a matrix form as

$$G^{\rm r}_\sigma(\omega) = \begin{bmatrix} g^{-1}_{1\sigma} & -t^*_1 & 0 & \cdots & {\rm i}\Gamma_{1N} \\ -t_1 & g^{-1}_{2\sigma} & -t^*_2 & 0 & \vdots \\ & & \ddots & & \\ \vdots & 0 & -t^*_{N-2} & g^{-1}_{N-1\sigma} & -t^*_{N-1} \\ {\rm i}\Gamma_{N1} & \cdots & 0 & -t_{N-1} & g^{-1}_{N\sigma} \end{bmatrix}^{-1}. \tag{3}$$

Here

$$g_{j\sigma} = [(z-\varepsilon_j)S_{j\sigma} + {\rm i}\Gamma_{jj}]^{-1},$$
$$S_{j\sigma} = \frac{z-\varepsilon_j-U_j}{z-\varepsilon_j-U_j+U_j\langle n_{j\bar\sigma}\rangle}. \tag{4}$$

The $g_{j\sigma}$ is the zero-order Green function of QD-j unperturbed by the other QDs with $z = \omega + {\rm i}0^+$ and $\Gamma_{ij} = \frac{1}{2}(\Gamma^{\rm L}_{ij} + \Gamma^{\rm R}_{ij})$, and $S_{j\sigma}$ arises from the second-order approximation for the Coulomb interaction [28, 30]. Notice that Γ_{jj} will become zero for the cases of $j \neq 1$ or N. The average electron occupation number in QDs is determined by the relations $\langle n_{j\sigma}\rangle = \frac{1}{2\pi}\int {\rm d}\omega\,{\rm Im}\,G^<_{jj,\sigma}$.

For the noninteracting case, it should be noted that the linear conductance spectrum of the coupled QD structure reflects the eigenenergy spectrum of the molecule made up of the coupled QDs. In other words, each resonant peak in the conductance spectrum represents an eigenenergy of the total QD molecule, rather than the levels of the individual QDs. Therefore, it is necessary to transform the Hamiltonian into the molecular orbital representation of the QDs. It is quite helpful to analyze the numerical results of the linear conductance spectrum.

We now introduce the electron creation (annihilation) operators corresponding to the molecular orbits, i.e. $f^\dagger_{j\sigma}(f_{j\sigma})$. By diagonalization of the single-particle Hamiltonian of the coupled QDs, we find the relation between the molecular and atomic representations (here each QD is regarded as an 'atom'). It is expressed as $[\boldsymbol{f}^\dagger_\sigma] = [\boldsymbol{\eta}][\boldsymbol{d}^\dagger_\sigma]$. The $N\times N$ transfer matrix $[\boldsymbol{\eta}]$ consists of the eigenvectors of the QD Hamiltonian. In the molecular orbital representation, the single-particle Hamiltonian takes the form $H = \sum_{k\sigma\alpha\in{\rm L,R}}\varepsilon_{\alpha k}c^\dagger_{\alpha k\sigma}c_{\alpha k\sigma} + \sum_{j=1,\sigma} e_j f^\dagger_{j\sigma}f_{j\sigma} + \sum_{\alpha k\sigma} v_{\alpha j}f^\dagger_{j\sigma}c_{\alpha k\sigma} + {\rm h.c.}$, in which e_j is the eigenenergy of the QDs. The coupling between the molecular state $|j\sigma\rangle$ and the state $|k\sigma\rangle$ in lead-α can be expressed as

$$v_{\alpha j} = V_{\alpha 1}[\boldsymbol{\eta}]^\dagger_{1j} + V_{\alpha N}[\boldsymbol{\eta}]^\dagger_{Nj}. \tag{5}$$

In the case of symmetric QD–lead coupling, the above relation can be rewritten as $v_{\alpha j} = V([\boldsymbol{\eta}]^\dagger_{1j} + [\boldsymbol{\eta}]^\dagger_{Nj}{\rm e}^{{\rm i}\phi_\alpha})$. Figure 1(b) shows the illustration of the QD structure in the molecular orbital representation. We can define $\gamma^\alpha_{jl} = 2\pi v_{\alpha j}v^*_{\alpha l}\rho_\alpha(\omega)$ which is the characteristic quantity that reflects the couplings between the molecule states and leads.

3. Numerical results and discussions

With the formulation developed above, we can perform the numerical calculation for the linear conductance spectra of the multi-QD system. Prior to the calculation we need to introduce a parameter t_0 as the unit of energy and take the Fermi level $\varepsilon_{\rm F}$ as the zero point of energy.

3.1. The triple-QD structure

The electron properties of the 2-QD structure, just the parallel-coupled double QDs, have received much attention during recent years [19, 20]. To begin with, we take the triple-QD structure to investigate the electron transport process without considering the many-body terms. As a typical case, we choose the parameter values $t_j = t_0$ for all QDs and $\Gamma^\alpha_{jj} = \Gamma$ to perform the numerical calculation; ε_j, the quantum-dot level, can be shifted with the adjustment of gate voltage. Figure 2 shows the numerical results of the linear conductance in the absence of a magnetic field. From this figure we find that in the case of $\varepsilon_j = \varepsilon_0$ (see the solid line in figure 2(a)), two conductance peaks appear in the conductance curve, consistent with the positions where $e_1 = \varepsilon_0 - \sqrt{2}t_0$ and $e_3 = \varepsilon_0 + \sqrt{2}t_0$ are both equal to zero. But there is no peak corresponding to the position of the eigenenergy $e_2 = \varepsilon_0 = 0$. In contrast, at this point the conductance presents its zero. In order to obtain a clear physical picture, we analyze this problem in the molecular orbital representation. By solving the $[\boldsymbol{\eta}]$ matrix and utilizing the relation $v_{\alpha j} = V([\boldsymbol{\eta}]^\dagger_{1j} + [\boldsymbol{\eta}]^\dagger_{Nj})$, one can find in such a case that $v_{\alpha 2}$ is fixed at zero, which brings out the complete decoupling of the second molecule state $|2\sigma\rangle$ from the leads and the formation of BIC. After a further analysis,

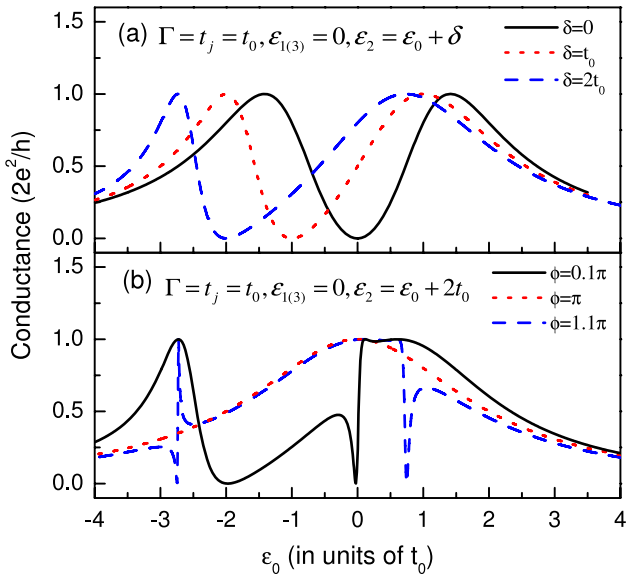

Figure 2. The linear conductance spectra of a triple-QD structure. The structure parameters take the following values: $\Gamma = t_j = t_0$ and $\varepsilon_1 = \varepsilon_3 = \varepsilon_0$. (a) for the cases of $\varepsilon_2 = \varepsilon_0 + \delta$ with δ equal to 0, t_0, and $2t_0$. (b) The conductances in the case of $\phi_L = \phi_R = \phi$ with $\phi = 0.1\pi$, π, and 1.1π.

we find that under the condition of $\varepsilon_1 = \varepsilon_3 = \varepsilon_0$, irrelevant to ε_2, $v_{\alpha 2}$ is always equal to zero, since the $[\eta]$ matrix is given by

$$[\eta] = \frac{1}{\sqrt{2\Delta}} \begin{bmatrix} \frac{2t_0}{\sqrt{\Delta-\delta}} & -\sqrt{\Delta-\delta} & \frac{2t_0}{\sqrt{\Delta-\delta}} \\ -1 & 0 & 1 \\ \frac{2t_0}{\sqrt{\Delta+\delta}} & \sqrt{\Delta+\delta} & \frac{2t_0}{\sqrt{\Delta+\delta}} \end{bmatrix} \tag{6}$$

with $\varepsilon_2 = \varepsilon_0 + \delta$ and $\Delta = \sqrt{\delta^2 + 8t_0^2}$. Thus the feature of QD-2 is not the necessary condition to cause the occurrence of BIC in electron tunneling through this structure. But the increase of δ gives rise to $\gamma_{11} \gg \gamma_{33}$, then a 'more' resonant state and a 'less' resonant state are constructed and Fano interference occurs between the coupled molecule states, corresponding to the case of $\delta = 2t_0$ in figure 2(a). In this figure, it is clear that the BIC phenomena are robust despite the change of the conductance lineshape. After these discussions, it is desirable to clarify the position of the antiresonant point in the linear conductance spectra. Based on the results in figure 2(a), we can see an interesting result that for the case of $\varepsilon_2 = 0$ the conductance becomes zero. That is to say, for such a configuration antiresonance always occurs when ε_2 is aligned with the Fermi level of the structure. Besides, with the help of equation (2), the expression for the conductance, such a result can be analytically obtained.

The underlying physics responsible for antiresonance is quantum interference. In order to clarify its mechanism, we analyze the electron transmission in the molecular orbital representation. Due to decoupling, only the molecule states $|1\sigma\rangle$ and $|3\sigma\rangle$ couple to the leads, which can also be called the bonding and antibonding states. To our knowledge, the molecular orbits of coupled double-QD structures, e.g. the well-known T-shaped QDs, are regarded as the bonding and antibonding states. Then, by representation transformation $[a_\sigma^\dagger] = [\boldsymbol{\beta}][f_\sigma^\dagger]$, such a configuration is changed into the T-shaped double-QD system (see figure 1(c)) of the Hamiltonian $\mathcal{H} = \sum_{k\sigma\alpha\in L,R} \varepsilon_{\alpha k} c_{\alpha k\sigma}^\dagger c_{\alpha k\sigma} + \sum_{\sigma,j=1}^{2} E_j a_{j\sigma}^\dagger a_{j\sigma} + \tau_1 a_{2\sigma}^\dagger a_{1\sigma} + \sum_{\alpha k\sigma} w_{\alpha 1} a_{1\sigma}^\dagger c_{\alpha k\sigma} + \text{h.c.}$. By a straightforward derivation, the relations between the structure parameters of the two configurations are expressed as $E_1 = \varepsilon_0$, $E_2 = \varepsilon_2$, $\tau_1 = \sqrt{2}t_0$, and $w_{\alpha 1} = V_{\alpha 1}$, respectively. Accordingly, we have $\gamma_{11}^\alpha = \Gamma|[\boldsymbol{\beta}]_{11}|^2$ and $\gamma_{33}^\alpha = \Gamma|[\boldsymbol{\beta}]_{12}|^2$ with $[\boldsymbol{\beta}] = \frac{1}{\sqrt{2\Delta}} \begin{bmatrix} \frac{2t_0}{\sqrt{\Delta-\delta}} & \frac{2t_0}{\sqrt{\Delta+\delta}} \\ \sqrt{\Delta+\delta} & -\sqrt{\Delta-\delta} \end{bmatrix}$. So the triple-QD structure is transformed into a T-shaped double QD with ε_2 being the level of the dangling QD. As discussed in previous works [15, 17, 28], in the T-shaped QDs antiresonance always occurs when the dangling QD level is the same as the Fermi level of the system. On the basis of such an analysis, one can then understand that in this triple-QD system the antiresonant point in the conductance spectrum is always consistent with the position of $\varepsilon_2 = \varepsilon_F = 0$.

The occurrence of antiresonance in the T-shaped QDs can be interpreted as the quantum interference between two kinds of transmission paths. We demonstrate this issue by rewriting the Hamiltonian of the T-shaped double-QD structure as $\mathcal{H} = \mathcal{H}_0 + \mathcal{H}_t$ in which

$$\begin{aligned} \mathcal{H}_0 = &\sum_{p\sigma} \xi_{Lp} \alpha_{Lp\sigma}^\dagger \alpha_{Lp\sigma} + \sum_{pk\sigma} (t_{pk} \alpha_{Lp\sigma}^\dagger c_{Rk\sigma} + \text{h.c.}) \\ &+ \sum_{k\sigma} \varepsilon_{Rk} c_{Rk\sigma}^\dagger c_{Rk\sigma} + \sum_{\sigma} \varepsilon_2 a_{2\sigma}^\dagger a_{2\sigma}, \\ \mathcal{H}_t = &\sum_{p\sigma} \mathcal{V}_p \alpha_{Lp\sigma}^\dagger a_{2\sigma} + \text{h.c.}. \end{aligned} \tag{7}$$

Here the old operators $a_{1\sigma}$ and $c_{Lk\sigma}$ are expanded in terms of this new set: $a_{1\sigma} = \sum_p v_p \alpha_{Lp\sigma}$ and $c_{Lk\sigma} = \sum_p v_{kp} \alpha_{Lp\sigma}$. Under this new representation, the electron transmission is well described: one represents an electron transmission path whereby the electron starts from the left lead and tunnels directly into the right lead, the other is a different transmission path in that the electron wave must visit the dangling QD as it tunnels through the QD structure. Note that the electron wave visiting the dangling QD will result in its phase change, and the phase difference between the two kinds of path gives rise to destructive quantum interference. A detailed discussion is presented in [30].

Next we investigate the modulation of magnetic field on the formation of BICs and antiresonance in electron transport through these structures. Here, we are interested in the case of equal magnetic flux through each subring, i.e. $\phi_L = \phi_R = \phi$. To present a generalized situation, the QD levels are assumed to be $\varepsilon_{1(3)} = \varepsilon_0$ and $\varepsilon_2 = \varepsilon_0 + 2t_0$, respectively. When a small magnetic flux is applied, a new Fano lineshape comes into being in the vicinity of the Fermi level, as shown by the solid line in figure 2(b). This is because the originally decoupled molecule state $|2\sigma\rangle$ begins to couple to the leads with a small state–lead coupling strength (in comparison with γ_{11} and γ_{33}), which causes the disappearance of BIC but offers a resonant channel for the Fano interference. With the increase of magnetic flux to $\phi = \pi$, the conductance curve shows itself as a Breit–Wigner lineshape and the position of its peak coincides with the Fermi level. It can be anticipated

that the first and third molecule states decouple from the lead simultaneously and only the second molecule state couples to the leads. Based on the discussion in the above section, in the presence of a magnetic flux the coupling between the molecule state $|j\sigma\rangle$ and lead-α takes the form $v_{\alpha j} = V([\boldsymbol{\eta}]^{\dagger}_{1j} + [\boldsymbol{\eta}]^{\dagger}_{Nj}e^{i\phi})$, by which one can clarify the results of $v_{\alpha 1(3)} = 0$ and $v_{\alpha 2} = \sqrt{2}V$ in the case of $\phi = \pi$. Therefore, in such a case there exist two bound states in the electron transport process, and the occurrence of BICs is more striking in comparison with the case of zero magnetic flux.

In the following we incorporate the many-body effect into the calculation of the conductance spectrum within the second-order approximation to truncate the equation of motion of the Green functions. Since the level of QD-2 is associated with the antiresonance in the noninteracting case, we first consider that the many-body term only exists in QD-2. Figure 3(a) exhibits the calculated conductances with $U_2 = 2t_0$ and $U_{1(3)} = 0$. It shows that in the absence of magnetic flux, there appear two antiresonant points in the conductance curve, corresponding to the positions of $\varepsilon_0 = 0$ and $-2t_0$. This is because the Coulomb repulsion splits the level of QD-2 ε_2 into ε_2 and $\varepsilon_2 + U_2$. As a consequence, whichever level of QD-2 is aligned with the Fermi level antiresonance still occurs. This means that in such a case the Coulomb interaction cannot destroy the occurrence of antiresonance. Besides, it is clear that in the case of magnetic flux $\phi = \pi$ the conductance spectrum shows itself as a Breit–Wigner lineshape with its peak at $\varepsilon_0 = 0$, identical with the noninteracting case. By virtue of representation transformation, such a result can be readily explained—the characteristics of the second molecule state, including its level and the state-lead coupling, are only determined by the features of QD-1 and QD-3 in the 'atomic' representation. Since in the case of $\phi = \pi$ only the second molecule state couples to the leads, it is understandable that the many-body effect in QD-2 makes zero contribution to the electron travel. By comparing the conductance spectra, we can readily find that the many-body effect in QD-2 is not able to restrain the formation of BICs, because in the absence of magnetic flux the conductance peak disappears at the position of $\varepsilon_0 = 0$ and in the case of $\phi = \pi$ the conductance spectrum just presents one resonant peak at the point of $\varepsilon_0 = 0$.

Figure 3(b) shows the calculated conductance spectra by considering the on-site energies of all the QDs $U_j = U = 2t_0$ and incorporating the many-body effect to the second order. The conductance spectra herein split into two groups due to Coulomb repulsion. But in each group the appearances of BICs and antiresonance are similar to the case of zero Coulomb interaction. In addition, between the two separated groups there is antiresonance fixed in the conductance spectra. Notice that unlike the conventional electron–hole symmetry, the position of such a conductance zero departs from $\varepsilon_0 = -\frac{U}{2}$. We can readily explain this phenomenon: because of the formation of BICs the average electron occupation numbers in the QDs are changed, as shown in figure 3(c). Thus, around the point of $\varepsilon_0 = -\frac{U}{2}$, the average electron occupation number $\langle n_{j\sigma}\rangle$ is no longer equal to $\frac{1}{2}$ and the electron–hole symmetry is broken by the presence of BICs [31]. In this sense we can understand that the BIC phenomenon causes the

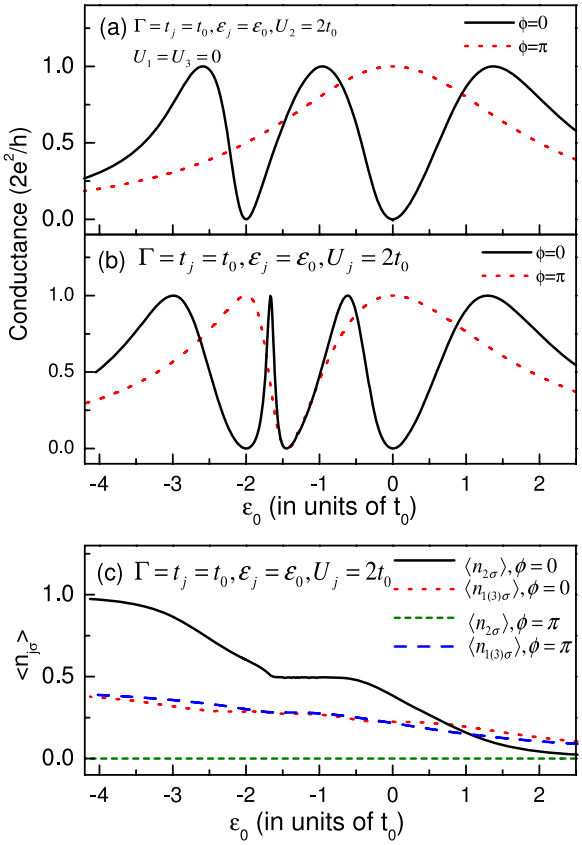

Figure 3. The conductance in the presence of the many-body effect with $\phi = 0$ and π. (a) The conductance in the case of $U_2 = 2t_0$ and $U_1 = U_3 = 0$. (b) The conductance spectra with $U_j = U = 2t_0$. (c) The average electron number in each QD under the condition of (b).

breaking of electron–hole symmetry under the second-order approximation.

3.2. Multi-QD structures

In this section we consider whether the electron transport properties of this structure show new phenomena with the further increase of QD number. As a typical case, the structure parameters take the values as $\Gamma_{jj} = \Gamma$, $t_j = t_0$, $\phi_\alpha = \phi$, and $\varepsilon_j = \varepsilon_0$, respectively, for the numerical calculation. Then the eigenenergies of the N-QD structure are given by $e_j = \varepsilon_0 - 2t_0\cos(\frac{j\pi}{N+1})$ and

$$[\boldsymbol{\eta}] = \sqrt{\frac{2}{N+1}} \times \begin{bmatrix} \sin\frac{N^2\pi}{N+1} & \sin\frac{N(N-1)\pi}{N+1} & \cdots & \sin\frac{N\pi}{N+1} \\ \sin\frac{N(N-1)\pi}{N+1} & \sin\frac{(N-1)^2\pi}{N+1} & \cdots & \sin\frac{(N-1)\pi}{N+1} \\ \vdots & & & \vdots \\ \sin\frac{N\pi}{N+1} & \sin\frac{(N-1)\pi}{N+1} & \cdots & \sin\frac{\pi}{N+1} \end{bmatrix}.$$

By analyzing this matrix, we can see that in the case of odd N,

$$[\boldsymbol{\eta}]^{\dagger}_{1j} = \begin{cases} [\boldsymbol{\eta}]^{\dagger}_{Nj}, & j \in \text{odd} \\ -[\boldsymbol{\eta}]^{\dagger}_{Nj}, & j \in \text{even}; \end{cases} \tag{8}$$

but in the presence of the even N, the opposite results will come about, i.e.

$$[\eta]^{\dagger}_{1j} = \begin{cases} -[\eta]^{\dagger}_{Nj}, & j \in \text{odd} \\ [\eta]^{\dagger}_{Nj}, & j \in \text{even}. \end{cases} \tag{9}$$

On the other hand, the coupling strength between the molecule state $|j\sigma\rangle$ and lead-α takes the form $v_{\alpha j} = V([\eta]^{\dagger}_{j1} + e^{i\phi}[\eta]^{\dagger}_{Nj})$. With the help of this relation, we can ascertain which molecule state decouples from the leads and becomes a bound state for the various QD structures. Correspondingly, in the absence of magnetic flux all even-molecule states decouple from the leads for the odd-numbered QD structures, but all odd-molecule states will decouple from the leads in the even-numbered QD systems. In figure 4(a) we plot the conductance spectra of the multi-QD structures ($N = 3$–6) with the shift of QD level. From the figure we can find the distinct occurrence of BICs. Taking the $N = 4$ case as an example, only two peaks appear in the conductance spectra corresponding to the eigenenergies e_2 and e_4, and the two molecule states ($|1\sigma\rangle$ and $|3\sigma\rangle$) completely decouple from the leads. Alternatively, when the magnetic flux is taken into account with $\phi = \pi$, this phenomenon will be modified thoroughly, as shown in figure 4(b). Here, unlike the zero magnetic flux cases, in the case of odd-numbered QDs the odd-molecule states decouple from the leads, and the even-molecule states decouple from the leads for the even-numbered QD systems. Therefore, one can find that in such a structure the bound states arise alternately with the adjustment of magnetic flux. By virtue of the above analysis, we can conclude that the emergence of BICs is tightly related to the space inversion symmetry of the system. And such space inversion symmetry leads to the compact form of the $[\eta]$ matrix and the well-regulated relationships between the elements of the matrix.

After the investigation of the BICs in electron transmission through the coupled QDs, it is necessary for us to ascertain the characteristic of antiresonance with increase in QD number. By comparing the numerical results in figure 4(a), the cases of zero magnetic flux, we find that the antiresonant points in the conductance spectra are just associated with the eigenenergies of QD molecules in which the peripheral QDs decouple from the other ones. For instance, the eigenenergies of the sub-molecule of the four-QD structure are $e'_1 = \varepsilon_0 - t_0$ and $e'_2 = \varepsilon_0 + t_0$. As a result, it is found that the e'_2 aligned with the Fermi level brings out the appearance of antiresonance. In addition, in the case of $N = 5$, the eigenlevels of its sub-molecule are $e'_1 = \varepsilon_0 - \sqrt{2}t_0$, $e'_2 = \varepsilon_0$ and $e'_3 = \varepsilon_0 + \sqrt{2}t_0$. We can find that when e'_1 or e'_3 is equal to zero, the electron transport shows itself as antiresonance. It seems that the antiresonant points are consistent with all even(odd) eigenenergies of the sub-molecule of the even(odd)-numbered QDs. Accordingly, there is a need to validate the correctness of such a prediction. It is certain that when the molecule state $|j\sigma\rangle$ couples to the leads then $\gamma^{\alpha}_{jj} = \Gamma|2[\eta]^{\dagger}_{1j}|^2$. Similar to the discussion on the triple-QD structure, such a relation can also be allowed to originate from the T-shaped QD structure by considering $|[\boldsymbol{\beta}]_{1l}| = |2[\eta]^{\dagger}_{1j}|$. Thereby, e_j is just the lth eigenlevel of the coupled T-shaped QDs. We hence can say that these two structures are equivalent to each other, and the parallel

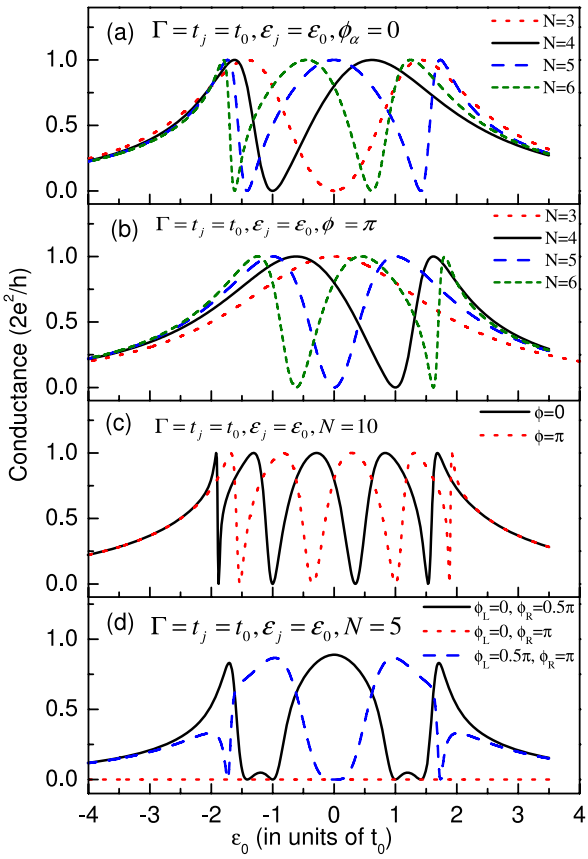

Figure 4. The conductance spectra with an increase in QD number. The structure parameters take the values $\Gamma = t_j = t_0$ and $\varepsilon_j = \varepsilon_0$. (a), (b) The conductances in the cases where N is increased from 3 to 6 in the absence or presence of magnetic flux. In (c) the 10-QD structure is investigated.

multi-QD system can be transformed into a T-shaped QD structure by representation transformation. Since the electron transport properties of the T-shaped QD structure are clear and characterized by antiresonance, we can conclude that in electron transport through this parallel multi-QD structure, antiresonance will inevitably occur. Furthermore, the structure parameters of the corresponding T-shaped QDs can be obtained because the $[\boldsymbol{\beta}]$ matrix and the eigenenergies are known. For instance, with respect to the five-QD system, we can see that in the absence of magnetic flux only the first, third, and fifth molecule states couple to the leads because of decoupling. Meanwhile, with the analysis of the $[\eta]$ matrix we can obtain $[\boldsymbol{\beta}] = 2\sqrt{\frac{2}{5}}[\sin\frac{\pi}{6}, \sin\frac{\pi}{2}, \sin\frac{\pi}{6}]^{\mathrm{T}}$ in such a case. Then, the corresponding T-shaped QD structure is well defined, as shown in figure 1(d). And the structure parameters take the values as $E_1 = \varepsilon_0$, $E_2 = \varepsilon_0 - \sqrt{2}t_0$, and $E_3 = \varepsilon_0 + \sqrt{2}t_0$ with the interdot coupling strengths $\tau_1 = \tau_2 = \frac{t_0}{\sqrt{2}}$. The origin of the antiresonance in the T-shaped system can be well understood, so in this multi-QD structure the occurrence of antiresonance in the electron transport process is ascertained. On the other hand, we can see that the modulation of the magnetic flux through the interferometer can efficiently change the appearance of antiresonance, namely, the antiresonant points are the same as all even(odd) eigenlevels of the sub-molecule of the odd(even)-

numbered QDs, as shown in figure 4(b). Besides, the results in figure 4(c), describing the case of ten QDs, support our predication. So, the electron transport properties in this system, involving the formation of BICs and antiresonance, have been clarified.

Now we focus on the case of $\phi_\alpha = n\pi$ and $\phi_{\alpha'} \neq n\pi$ where some molecule states of the coupled QDs decouple from lead-α but couple to lead-α'. Thereby, in such a case one will not find the BIC phenomena, since there is no probability of $\Gamma_{jj} = 0$. However, one will see the striking antiresonance in electron tunneling through the structure. Correspondingly, there are two kinds of antiresonant points in the conductance spectra. First, with respect to the odd-numbered QD structures, when $\phi_\alpha = (2n-1)\pi$ and $\phi_{\alpha'} \neq n\pi$ the odd-molecule state $|2j-1,\sigma\rangle$ will decouple from lead-α, and such a kind of decoupling can result in antiresonance at the positions of $e_{2j-1} = 0$. In addition, the couplings between all even-molecule states and the leads offer channels for electron tunneling, and the quantum interference among electron waves passing through these channels also causes antiresonance. As discussed above, these zero points of the conductance are consistent with the even eigenenergies of the sub-molecule of the whole QD structure. As shown by the dashed line in figure 4(d) with $\phi_{\rm L} = 0.5\pi$ and $\phi_{\rm R} = \pi$, there are three antiresonances corresponding to the positions of e_1, e_3, and $e_5 = 0$, respectively. Besides, in the case of $e'_2 = 0$ the electron transport shows antiresonance. It should be pointed out that due to $e_3 = e'_2$ the antiresonance valley around the point of $\varepsilon_0 = 0$ is broadened [28]. On the other hand, in the case of $\phi_\alpha = 2n\pi$ and $\phi_{\alpha'} \neq n\pi$ the even-molecule states will decouple from lead-α but all odd-molecule states couple to both leads. The solid line in figure 4(d) describes this situation with $\phi_{\rm L} = 0$ and $\phi_{\rm R} = 0.5\pi$. Obviously, two antiresonant points correspond to the points of $e_{2(4)} = 0$, since the molecule states $|2\sigma\rangle$ and $|4\sigma\rangle$ decouple from lead-L. Meanwhile, the other antiresonances, from the quantum interference among the odd-molecule states, coincide with the cases of $e'_{1(3)} = 0$. By a same token, the electron transport properties of the even-numbered QD structure can also be analyzed, which will be opposite to those in the odd-numbered QD systems.

Based on the results of decoupling in electron transport through this kind of structure, one can expect that when a finite bias is applied on the system, a negative differential capacitance will emerge [32]. In figure 5 we plot the curves of the average occupation number of electrons in the QDs with increase in the bias voltage. Obviously, the figure shows that the average occupation number of electrons in QDs decreases with the increase of bias voltage, which indicates the appearance of negative differential capacitance. We can illustrate such a phenomenon as follows. When a finite bias is applied on the system, the QD levels can be adjusted by the bias voltage. They are not aligned with each other, since these QDs are located at different positions of the electrostatic potential induced by the bias voltage [30]. As a consequence, the decoupling phenomenon can be demolished since the structure parameters that take some specific values are destroyed by the variation of the bias voltage. Thus, the electrons located in QDs due to the decoupling effect, driven by the bias, will take part in electron tunneling and then enter the drain of the system. With such an analysis, one can understand the negative differential capacitance driven by the bias voltage.

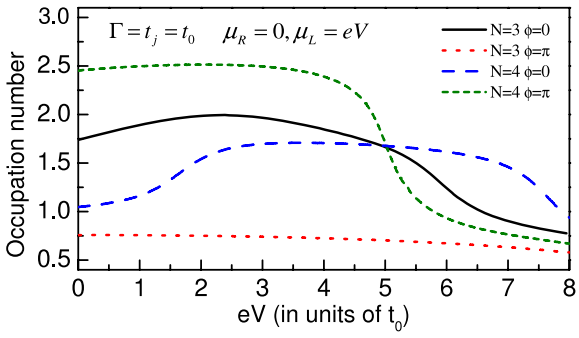

Figure 5. The average electron occupation number in the QDs with the increase of bias voltage. The parameters used in the calculation are: $\Gamma = t_j = t_0$, $\mu_{\rm R} = 0$, $\mu_{\rm L} = eV$, and the bandwidths of the leads are taken as $5t_0$. To simulate the dependence of the QD levels on the bias, we take $\varepsilon_1 = \varepsilon_N = \frac{1}{2}eV$ and the levels of the other QDs as $\frac{1}{4}eV$.

Finally we should emphasize the following point about the many-body term. Based on the calculation of the triple-QD structure, we can predict that when the Coulomb repulsions are taken into account within the second order, the single-electron transport properties will remain although the conductance spectra are divided into two groups. However, in the strong correlation regime the Kondo resonance must modify the linear conductance spectrum when the QD levels are far below the Fermi energy [33]. Such an interesting topic is beyond the scope of the present work, and will be left for future study.

4. Summary

With the help of the nonequilibrium Green function technique, we have theoretically investigated the electronic transport properties in a multi-QD system, in which a one-dimensional QD chain is embodied in a Aharonov–Bohm interferometer with the peripheral QDs in its two arms. As a result, we have found the remarkable BIC phenomenon and antiresonance in the process of electron transport. That is to say, as for the odd-numbered QD structures, in the absence of magnetic flux all even-molecule states of the QDs decouple from the leads, whereas the odd-molecule states decouple from the leads for the even-numbered QD systems. On the other hand, the antiresonant points in the conductance spectra are consistent with the even(odd) eigenlevels of the sub-molecule of the even(odd)-numbered QD structures in the absence of peripheral QDs. By representation transformation, these results are analyzed in detail. Besides, it has been found that with the presence of magnetic flux through the interferometer, the appearance of BICs and antiresonance is completely modified. Furthermore, by adjusting the magnetic flux through any subring of the structure, some molecule states decouple from one lead but still couple to the other, which leads to the occurrence of new antiresonance. These properties remain when the many-body effect due to the intradot electron interaction is taken into account.

It should be noted that the research into BICs originated from aspects of atomic and molecular physics, and it is of importance for the study of quantum information [14, 23]. Two simultaneous BICs could be used as microscopic units for storing information, since the storage of quantum information requires a complete stable plane in the Hilbert space of the molecule. Coupled QDs, also called artificial molecules, are the suitable systems for the experimental study of BICs due to the possibility of adjusting their structure parameters; we thus expect that the calculated results in this work could be helpful for the current experiments.

Acknowledgment

This work was financially supported by the National Natural Science Foundation of China under grant no. NNSFC10847109.

References

[1] von Neumann J and Wigner E 1929 *Phys. Z.* **30** 465
[2] Stillinger F H and Herrick D R 1975 *Phys. Rev.* A **11** 446
[3] Fonda L and Newton R G 1960 *Ann. Phys. NY* **10** 490
Vanroose W 2001 *Phys. Rev.* A **64** 062708
Longhi S 2007 *Eur. Phys. J.* B **57** 45
[4] Friedrich H and Wintgen D 1985 *Phys. Rev.* A **31** 3964
[5] Rzążewski K, Lewenstein M and Eberly J H 1982 *J. Phys. B: At. Mol. Phys.* **15** L661
John S and Wang J 1990 *Phys. Rev. Lett.* **64** 2418
John S and Wang J 1991 *Phys. Rev.* B **43** 12772
[6] Kofman A G, Kurizki G and Sherman B 1994 *J. Mod. Opt.* **41** 353
Wang X H, Gu B Y, Wang R and Xu H Q 2003 *Phys. Rev. Lett.* **91** 113904
[7] Miyamoto M 2005 *Phys. Rev.* A **72** 063405
[8] Wang X R 1995 *Phys. Rev.* B **51** 9310
Wang X R 1996 *Phys. Rev.* B **53** 12035
[9] Capasso F, Sirtori C, Faist J, Sivco D L, Chu S-N G and Cho A Y 1992 *Nature* **358** 565 and the references therein
[10] Schult R L, Wyld H W and Ravenhall D G 1990 *Phys. Rev.* B **41** 12760
[11] Ji Z-L and Berggren K-F 1992 *Phys. Rev.* B **45** 6652
[12] Deo P S and Jayannavar A M 1994 *Phys. Rev.* B **50** 11629
[13] Voo K-K and Chu C S 2006 *Phys. Rev.* B **74** 155306
[14] Ordonez G, Na K and Kim S 2006 *Phys. Rev.* A **73** 022113
[15] Wang X R, Wang Y and Sun Z Z 2002 *Phys. Rev.* B **65** 193402
[16] Tanaka S, Garmon S, Ordonez G and Petrosky T 2007 *Phys. Rev.* B **76** 153308
[17] Kobayashi K, Aikawa H, Katsumoto S and Iye Y 2002 *Phys. Rev. Lett.* **88** 256806
Kobayashi K, Aikawa H, Katsumoto S and Iye Y 2003 *Phys. Rev.* B **68** 235304
Sato M, Aikawa H, Kobayashi K, Katsumoto S and Iye Y 2005 *Phys. Rev. Lett.* **95** 066801
[18] Kubala B and König J 2002 *Phys. Rev.* B **65** 245301
Golosov D I and Gefen Y 2006 *Phys. Rev.* B **74** 205316
[19] Orellana P A, Domínguez-Adame F, Gómez I and Ladrón de Guevara M L 2003 *Phys. Rev.* B **67** 085321
[20] Lu H, Lü R and Zhu B F 2005 *Phys. Rev.* B **71** 235320
Bai Z-M, Yang M-F and Chen Y-C 2004 *J. Phys.: Condens. Matter* **16** 4303
Kang K and Cho S Y 2004 *J. Phys.: Condens. Matter* **16** 117
[21] Sun Q-F, Wang J and Guo H 2005 *Phys. Rev.* B **71** 165310
[22] Ladrón de Guevara M L, Claro F and Orellana P A 2003 *Phys. Rev.* B **67** 195335
[23] Ladrón de Guevara M L and Orellana P A 2006 *Phys. Rev.* B **73** 205303
[24] Bao K and Zheng Y 2006 *Phys. Rev.* B **73** 045306
[25] Waugh F R, Berry M J, Mar D J and Westervelt R M 1995 *Phys. Rev. Lett.* **75** 705
[26] Sigrist M, Ihn T, Ensslin K, Reinwald M and Wegscheider W 2007 *Phys. Rev. Lett.* **98** 036805
[27] Chan W L, Wang X R and Xie X C 1996 *Phys. Rev.* B **54** 11213
[28] Gong W, Zheng Y, Liu Y and Lü T 2006 *Phys. Rev.* B **73** 245329
[29] Meir Y and Wingreen N S 1992 *Phys. Rev. Lett.* **68** 2512
Jauho A P, Wingreen N S and Meir Y 1994 *Phys. Rev.* B **50** 5528
[30] Liu Y, Zheng Y, Gong W and Lü T 2007 *Phys. Rev.* B **76** 195326
Liu Y, Zheng Y, Gong W and Lü T 2006 *Phys. Lett.* A **360** 154
[31] Han Y, Gong W, Wu H and Wei G 2009 arXiv:0902.2243v1 [cond-mat]
[32] Wang S D, Sun Z Z, Cue N, Xu H Q and Wang X R 2002 *Phys. Rev.* B **65** 125307
[33] Goldhaber-Gordon D, Shtrikman H, Mahalu D, Abusch-Magder D, Meirav U and Kastner M A 1998 *Nature* **391** 156
Kashcheyevs V, Aharony A and Entin-Wohlman O 2006 *Phys. Rev.* B **73** 125338